AMERICAN JOURNAL OF PHYSIOLOGY
ENDOCRINOLOGY AND METABOLISM

Am J Physiol Endocrinol Metab 323: E69–E79, 2022.
First published May 16, 2022; doi:10.1152/ajpendo.00293.2021

RESEARCH ARTICLE

Translational Physiology

Pantothenate protects against obesity via brown adipose tissue activation

Huiqiao Zhou,[1,2]* Hanlin Zhang,[1,2]* Rongcai Ye,[1,2]* Chunlong Yan,[3]* Jun Lin,[1,2] Yuanyuan Huang,[1] Xiaoxiao Jiang,[1,2] Shouli Yuan,[1,2] Li Chen,[1,2] Rui Jiang,[1,2] Kexin Zheng,[4] Ziyu Cheng,[1,2] Zhi Zhang,[1,2] Meng Dong,[1] and Wanzhu Jin[1,2]

[1]*Key Laboratory of Animal Ecology and Conservation Biology, Institute of Zoology, Chinese Academy of Sciences, Beijing, China;* [2]*University of the Chinese Academy of Sciences, Beijing, China;* [3]*College of Agriculture, Yanbian University, Yanji, China; and* [4]*Institutes of Infectious Diseases, Beijing Ditan Hospital, Capital Medical University, Beijing, China*

Abstract

Brown adipose tissue (BAT) is the primary site of adaptive thermogenesis, which is involved in energy expenditure and has received much attention in the field of obesity treatment. By screening a small-molecule compound library of drugs approved by the Food and Drug Administration, pantothenic acid was identified as being able to significantly upregulate the expression of uncoupling protein 1 (UCP1), a key thermogenic protein found in BAT. Pantothenate (PA) treatment decreased adiposity, reversed hepatic steatosis, and improved glucose homeostasis by increasing energy expenditure in C57BL/6J mice fed a high-fat diet. PA also significantly increased BAT activity and induced beige adipocytes formation. Mechanistically, the beneficial effects were mediated by UCP1 because PA treatment was unable to ameliorate obesity in UCP1 knockout mice. In conclusion, we identified PA as an effective BAT activator that can prevent obesity and may represent a promising strategy for the clinical treatment of obesity and related metabolic diseases.

NEW & NOTEWORTHY PA treatment effectively and safely protected against obesity via the BAT-UCP1 axis. PA has therapeutic potential for treating obesity and type II diabetes.

brown adipose tissue; obesity; pantothenate; pantothenic acid; uncoupling protein 1

INTRODUCTION

Changes in the standard of living have resulted in the emergence of increasingly unhealthy lifestyles, the excessive intake of nutrients, and the eventual development of obesity (1). Accumulating evidence indicates that obesity is the primary culprit underlying the development of type II diabetes, metabolic syndrome, insulin resistance, fatty liver, hypercholesteremia, hypertension, polycystic ovarian syndrome, inflammation, and cancer (2–6). Obesity is also associated with an increased risk of death and is reportedly the fifth-leading cause of death worldwide (7). Therefore, effective treatments for obesity both are essential and urgent.

Obesity develops in response to an imbalance in energy metabolism. Accordingly, limiting energy intake and increasing energy expenditure are the two basic methods for reducing obesity. In terms of limiting energy intake, diet restriction is the most common method for treating obesity but has poor sustainability. Increasing trials have attempted to develop appetite suppressors, including 5-hydroxytryptamine (5-HT) 2C receptor activators, which stimulate the central nervous system. The lipase inhibitor orlistat has also been developed to decrease gut lipid absorption and energy absorption (8). However, a series of side effects, including anorexia, nausea, and malnutrition, have hindered the application of these drugs for treating obesity (9).

Exercise therapy is the most common therapy for combatting obesity, which functions to increase energy expenditure. However, the weight-loss effect of exercise therapy is overestimated, and it requires long-term persistence and perseverance (10). Consequently, whether any other methods can be used to increase energy expenditure remains an important question. Recent studies have explored mechanisms for promoting body heat production and increasing energy expenditure to improve the balance in energy metabolism (11).

There is a reported negative relationship between body mass index and brown adipose tissue (BAT) (12). BAT burns fat to release heat for thermogenesis and represents an ideal target for treating obesity and diabetes (13). Fully activated BAT could respond to 20% of the basal human energy expenditure (14). A wide range of evidence suggests that specific dietary factors are critical for BAT activation and thermogenesis (15). In addition, beige adipocytes can

*H. Zhou, H. Zhang, R. Ye, and C. Yan contributed equally to this work.
Correspondence: W. Jin (jinw@ioz.ac.cn); M. Dong (dongmeng90@foxmail.com).
Submitted 18 August 2021 / Revised 9 May 2022 / Accepted 9 May 2022

be induced within white adipose tissue (WAT) by certain stimuli, in a process known as "browning" or "beiging" (16). Beige adipose tissue possesses a marked capacity for energy expenditure via thermogenesis (17). Our previous work revealed that food ingredients, such as ginseng extract, rutin (mulberry extract), and myricetin (a dietary flavonoid) can increase whole body energy expenditure via the activation of BAT and beige adipocytes formation (18–20). Safe approaches for the long-term use of food ingredients should be established to activate BAT for treating obesity in humans.

In this study, the Food and Drug Administration (FDA)-approved small-molecule compound library was screened for potential uncoupling protein 1 (UCP1) activators, and pantothenic acid was identified as a promising BAT activator. Pantothenic acid, also known as vitamin B_5, is a member of the vitamin B family found in foods, such as eggs, milk, and vegetables, and is primarily absorbed by the intestines (21). Pantothenic acid is involved in the Krebs cycle in its ionic form, pantothenate (PA), commonly as its alcohol analogs, provitamin panthenol, and calcium pantothenate. (22). Pantothenic acid and its pantothenate derivatives have been applied for dyslipidemia treatment for decades, and one of the derivatives of pantothenic acid, pantethine, has exhibited favorable effects in hyperlipemia (23, 24). However, previous studies have not confirmed any established benefits for pantothenic acid supplementation among overweight or obese adults, and the mechanisms of its action remain unknown. Pantothenic acid supplementation prevents calorie overload-induced free fatty acid toxicity and hyperglycemia, suggesting that, as a precursor of coenzyme A (CoA), PA is prominently involved in lipid metabolism (25).

In this study, we revealed that PA activates BAT both in vitro and in vivo. For the first time, to our knowledge, we reported that PA treatment can increase energy expenditure and thermogenesis via BAT activation, ultimately preventing obesity and inducing metabolic remodeling. Overall, PA treatment is a promising approach to preventing obesity.

METHODS

Mice

C57BL/6J mice (3 wk old, male) were purchased from Vital River Laboratories (Beijing, China). The UCP1 knockout (KO mice with C57/BL6J background) were obtained as a gift from L Kozak (Pennington Medical Research Center, Baton Rouge, LA). Both WT and UCP1KO mice were bred from UCP1 KO heterozygous littermates and genotyped as described previously (26). All mice were housed under 24°C and 55% ± 10% humidity with 12-h light-dark cycle in specific pathogen free (SPF) laboratory animal-house (Institute of Zoology of Beijing, Chinese Academy of Sciences, China). In thermoneutral experiments, mice were housed at a 30°C chamber with 12-h light-dark cycle. The normal chow diet is 11.7% fat and 10 μg/g of PA (MD17121, Medicience). High-fat diet (HFD) is 60% fat and 20 μg/g of PA (MD12033, Medicience). Water and diets were provided on the ad libitum basis. All the mice were anesthetized by isoflurane before being euthanized. All the animal studies were conducted with the approval of the Institutional Animal Care and Use Committee of the Institute of Zoology, Chinese Academy of Sciences. Investigators were blinded to allocation during experiments and data analysis with a power analysis of 0.8. No mice were excluded from the study during the experiment.

PA Treatment

D-pantothenic acid hemicalcium salt (P5155, Sigma) was dissolved in sterile saline (0.9% NaCl) for mouse experiments. To generate HFD mice groups, 3-wk-old mice were fed a normal chow diet for 3 wk, then shifted to an HFD and administered either PA (10 mg/kg body wt) or saline via oral gavage daily until euthanized. To generate corresponding no-HFD mouse groups, 3-wk-old mice were fed with a normal chow diet for 3 wk then maintained on that same diet and administered either PA (10 mg/kg body wt) or saline via oral gavage daily until euthanized All mice were weighed weekly. The rationale of dosage was based on an estimated conversion formula that assumes that 1 μM in cell culture medium equates to 0.6 mg/kg body wt in mouse serum. With respect to combatting obesity, the optimal concentration of PA was determined to be 10.0 mg/kg based on a preliminary test with concentrations of 0.6, 5.0, and 10.0 mg/kg (data not shown). No adverse reaction could be observed in mice with the above dosages. According to body surface area conversion, PA treatment in humans with a weight of 50 kg is $\sim$10 mg/kg $\times$ 0.0026 $\times$ 50 kg = 1.3 mg, which is within the safe dosage of 5 mg/kg in humans according to reported study (27).

Cell Experiment

Human primary brown adipocytes were a gift from Beijing Key Laboratory of Diabetes Prevention and Research, Lu He hospital. Isolation of human primary brown adipocytes was described previously and complied with the Declaration of Helsinki for investigation of human subjects (28). It was approved as ethical by the competent Institutional Review Boards of the Capital Medical University. Classical interscapular BAT-derived human primary brown adipocytes were cultivated in Dulbecco's modified eagle medium (DMEM) (high glucose, 450 mg/dL) containing 20% fetal bovine serum (FBS) (v/v), 20 mM HEPES, penicillin, and streptomycin. The fifth passage of the human primary brown adipocytes was treated with 626 compounds from FDA-approved drugs library (National Small Molecule Compound Resource Center), which are respectively resolved in DMSO and harvested in 24 h. For mouse brown adipocytes, brown stromal vascular fraction was isolated from C57BL/6J neonatal mice after isoflurane anesthesia and disinfected with 75% alcohol. Interscapular brown fat pad was separated and cut into small particles and minced, then transferred into a 1.5 mL tube containing 1 mL digestion buffer (1.5 mg/mL collagenase I) and incubated in a 37°C water bath for digesting. Culture medium (5 mL) stopped the digestion and filtered through a 100 μm nylon filter into a new 50 mL sterile tube. After centrifuging at room temperature at 600 *g* for 5 min, the stromal vascular fraction (SVF) pellets were resuspended and cultured in DMEM medium with 20% FBS incubating at 37°C and 5% CO_2. For brown adipocytes differentiation assays, 100%

confluent SVF was changed into the induction medium containing 0.5 mM 3-isobutyl-1- methylxanthine (IBMX), 2 μg/mL dexamethasone, 20 nM insulin, 1 μM rosiglitazone, 1 nM 3,3′,5-triiodo-l-thyronine (T3), and 0.125 mM indomethacin. On the third day, maintaining medium was applied, which contained 20 nM insulin, 1 μM Rosiglitazone, and 1 nM T3, and continued to the sixth day. PA was resolved in sterile distilled deionized water for mouse cell treatment. For mouse primary brown adipocytes differentiation assays, PA was treated for 6 days since the SVF cells were 100% confluent. Compound C (500 μM) (Selleck, S 7306) was applied on the sixth day of primary brown adipocytes differentiation for 2 h before harvest.

Oil Red O Staining

To detect lipid, differentiated mouse brown adipocytes were fixed with 4% paraformaldehyde and stained with 0.2% Oil Red O (Oil Red O; Sigma, Cat. No. 0–0625). These results were observed by an inverted microscope (DS-RI1; Nikon).

Histological Analysis

For hematoxylin-eosin (H&E) staining, tissues fixed with 4% paraformaldehyde were embedded in paraffin. Thick sections (5 μm) were stained and observed under ×20 objective lens.

Glucose Tolerance Test

At the 12th week, the mice were fasted overnight (17:00 h to 9:00 h) with free access to drinking water. Ten percent of D-glucose (w/v) was injected intraperitoneally (1.5 g/kg of body wt) and the blood glucose levels were measured by Accu-Chek glucose monitor (Roche Diagnostics Corp, 35 Pleasanton, CA) before and 15, 30, 60, 90, and 120 min after injection.

Body Composition Measurements

The lean and fat mass of mice were assessed with the Small Animal Body Composition Analysis and Imaging System (MesoQMR 23-060H-I, Nuimag Corp).

Metabolic Rate and Physical Activity

The oxygen consumption was measured with a TSE LabMaster (TSE Systems, Bad Homburg, Germany) as previously described (29). Mice were acclimated to the system and maintained at 24°C or 30°C under a 12-h light/dark cycle for 48 h, and had free access to food and water. $\dot{V}O_2$ or $\dot{V}CO_2$ of each mouse were obtained every 10 min. The O_2 consumption ($\dot{V}O_2$) data are presented as running mean curves, where each point is a running mean from 10-min periods). The voluntary activity of each mouse was measured with an optical beam technique (Opto-M3, Columbus Instruments, Columbus, OH) for 24 h and expressed as average activity.

Rectal Temperature Measurement

For cold exposure experiments, mice were placed in a cold chamber (4°C) for up to 2 h with free access to food and water. Body temperature was measured via a rectal probe connected to a digital thermometer (Yellow Spring Instruments) before cold exposure, and 1, 2 h after cold exposure. In mice subjected to induced thermogenesis via CL316,243(1 mg/kg) injection, rectal temperature was measured by the probe before and 15, 25 min after injection.

Real-Time Quantitative PCR

Total RNA from tissues and cells was extracted with Trizo Reagent (Thermo Fisher Scientific) and reverse-transcribed with high-capacity cDNA reverse transcription kit (R312-01/02, Vazyme). The relative expression of genes was detected by real-time fluorescence quantitative polymerase chain reaction (ABI Prism VIIA7; Applied Biosystems) Synergy Brands (SYBR) Green Master Mix (Q511-AA, Vazyme) and normalized by cyclophilin expression. All the sequences of primers were designed and downloaded from National Center for Biotechnology Information (NCBI) primer blast (https://www.ncbi.nlm.nih.gov/tools/primer-blast/). The list of primers was shown in Table 1.

Measurement of Citrate Synthase Activity

Citrate synthase (CS) activity was determined according to the manufacturer's instruction by measuring coenzyme A formation at 412 nm with Citrate Synthase Activity Assay Kit (Solarbio bc 1065, China) from differentiated mouse primary adipocytes, BAT and subcutaneous adipose tissue (SUB).

Western Blot

For relative protein expression level detection, a series of Western blot were performed. Briefly, total proteins of cells were extracted by radio immunoprecipitation assay (RIPA) buffer and tissue proteins were obtained by additional grinding with ULTRA-TURRAX handheld homogenizer (IKA, Germany). Then 25 μg of proteins of each sample were loaded in 10% SDS-polyacrylamide gels to get separated and transferred to PVDF membranes. In SUB Western blots of UCP1, 3 μg of proteins of BAT were loaded as active control. The proteins were incubated with the following antibodies for 12 h in 4°C: anti-UCP1 (Abcam, Cat. No. ab10983, RRID:AB_2241462,1:1,000, rabbit), PGC1α (Abcam, Cat. No. ab54481, RRID:AB_881987, 1:1,000, rabbit), P-AMPK (CST, Cat. No. 2535, RRID:AB_331250, 1:1,000, rabbit), AMPK (CST, Cat. No. 2603, RRID:AB_490795, 1:1,000, rabbit), anti-Tubulin (CST, Cat. No. 2146, RRID:AB_2210545, 1:1,000, rabbit), anti-HSP90 (CST, Cat. No. 4874, RRID:AB_2121214, 1:1,000, rabbit), P-Akt (CST, Cat. No. 9271, RRID:AB_329825, 1:1,000, rabbit), Akt (CST, Cat. No. 9272, RRID:AB_330713, 1:1,000, rabbit), P-P38(CST Cat. No. 4631, RRID:AB_331765, 1:1,000, rabbit), P38 (CST, Cat. No. 9212, RRID:AB_330713, 1:1,000, rabbit), P-PKA substrate (CST, Cat. No. 9621, RRID:AB_330304, 1:1,000, rabbit), OXPHOS (Abcam, Cat. No. ab110413, RRID:AB_26292, 1:500, mouse), P-ERK (CST Cat. No. 9101, RRID:AB_331646, 1:1,000, rabbit), ERK (CST, Cat. No. 9102, RRID:AB_330744, 1:1,000, rabbit), and TH (Abcam, Cat. No. ab137869, RRID:AB_2801410, 1:500, rabbit) were incubated with horseradish peroxidase (HRP)-conjugated secondary antibodies for 1h at room temperature: anti-mouse (Beyotime, Cat. No. A0216, RRID:AB_2860575,1:5,000) and anti-rabbit (Beyotime, Cat. No. A0208, RRID:AB_2892644,1:5,000). All the signals were visualized by densitometric scanning (Image Quant TL7.0; GE Healthcare Biosciences, Uppsala Sweden). Blots densitometry of the bands were analyzed via ImageJ software (National Institutes of Health, Bethesda, MD).

Table 1. *Primers for RT-PCR*

Gene	Forward	Reverse
Human-Cyclophilin	TAAAGCATACGGGTCCTGGC	GACTGAGTGGTTGGATGGCA
Human-UCP1	GCAGGGAAAGAAACAGCACC	CCCGTGTAGCGAGGTTTGAT
Mouse-Cyclophilin	CAAATGCTGGACCAAACACAA	GCCATCCAGCCATTCAGTCT
Mouse-UCP1	GGCAAAAACAGAAGGATTGC	TAAGCCGGCTGAGATCTTGT
Mouse-PPAR γ2	TCGCTGCTGCACTGCCTCTG	GAGAGGTCCACAGAGCTGATT
Mouse-PGC1α	ACAGCTTTCTGGGTGGATTG	TGAGGACCGCTAGCAAGTTT
Mouse-TFAM	GTCCATAGGCACCGTATTGC	CCCATGCTGGAAAAACACTT
Mouse-NRF1	CAACAGGGAAGAAACGGAAA	GCACCACATTCTCCAAAGGT
Mouse-NRF2	CCCCCGAGGACACTTCTTATG	AGCAGCCAGATGGGCAGTTA
Mouse-Dio2	GCCATGCCATGCAGTTAGGA	TTGGGAATTCGGGGCTACAG
Mouse-ADRβ1	GCCCTTTCGCTACCAGAGTT	ACTTGGGGTCGTTGTAGCAG
Mouse-ADRβ2	TGGTTGGGCTACGTCAACTC	CCAGCTGACAAGTGTTTGGC
Mouse-ADRβ3	AACTGGTTGCGAACTGTGGAq	CGTAACGCAAAGGGTTGGTG

Blood Analysis

Serum was separated and stored at −80°C. Enzyme-linked immunosorbent assay kits were applied to detect serum insulin concentration as per the manufacturer's instructions (Cusabio, Cat. No. CSB-E05071m).

Statistics

In figure legends, "*n*" stands for biological replications. Data are expressed as means ± SE. Statistics were performed using one-way analysis of variance (ANOVA) or Student's *t* test. Statistical significance was set at $P < 0.05$; $^{*}P < 0.05$, $^{**}P < 0.01$, and $^{***}P < 0.001$.

RESULTS

Pantothenate Increases UCP1 Expression and Promotes the Differentiation of Brown Adipocytes

Recently, our group screened an FDA-approved drug library and identified effective BAT activators in human brown adipocytes (hBAc) (30). Most of these small-molecule compounds

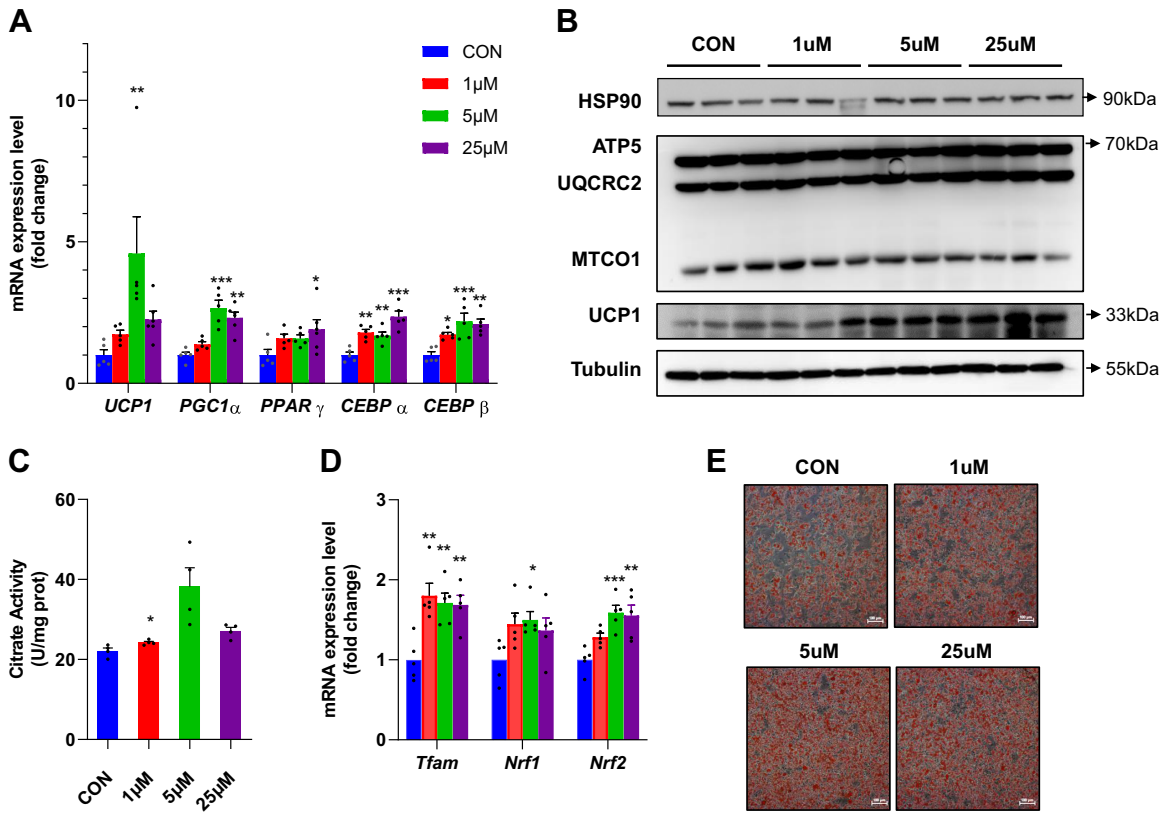

Figure 1. Pantothenate (PA) stimulates the activity and induces differentiation of brown adipocytes. *A*: mRNA expression levels of BAT marker genes (for each group, $n = 5$). *B*: Western blot of HSP90, OXPHOS, UCP1, and tubulin expression ($n = 3$). *B* and C: citrate synthase activity ($n = 4$). *D*: mRNA expression levels of mitochondrial biogenic genes ($n = 5$). *E*: oil staining of differentiated brown adipocytes treated with PA (0, 1, 5, and 25 μM) on *day 0* for 6 days. Data are shown as means ± SE. Statistical analysis was performed by one-way repeated-measures ANOVA (*A–D*) with multiple comparisons and Tukey's posttest; $^{***}P < 0.001$, $^{**}P < 0.01$, and $^{*}P < 0.05$ were considered significant. BAT, brown adipose tissue; HSP90, heat shock protein 90; OXPHOS, oxidative phosphorylation; UCP1, uncoupling protein 1.

AJP-Endocrinol Metab • doi:10.1152/ajpendo.00293.2021 • www.ajpendo.org

are antibiotics, hormones, or anticancer drugs with reported side effects. Capsicin and fluvastatin sodium have been reported to act as BAT activators (30, 31) (Supplemental Fig. S1; see https://doi.org/10.6084/m9.figshare.15180819.v8). Thus, pantothenic acid was identified as a promising small-molecule compound that upregulates UCP1 expression in hBAc (Supplemental Fig. Fig. S1). Pantothenic acid is a component of the hBAc differentiation cocktail, suggesting that it could serve as a BAT activator (30). As a pantothenic acid analog, PA serves as a CoA enzymatic component and possesses better solubility and absorption characteristics than pantothenic acid (32). Here, we treated mouse primary brown adipocytes with PA using a concentration gradient of 1, 5, and 25 μM for 6 days. The results showed that UCP1 was significantly upregulated after PA treatment (Fig. 1, *A* and *B*, and Supplemental Fig. S2*A*). As mitochondria are enriched in brown adipocytes, we investigated citrate synthase (CS) activity, which is a mitochondrial mass indicator. We found that CS activity was greatly increased by PA treatment (Fig. 1*C*). In addition, the expression levels of key genes involved in mitochondrial biogenesis, such as mitochondrial transcription factor A (*Tfam*), nuclear respiratory factor 1 (*NRF1*), and nuclear respiratory factor 2 (*NRF2*), were also increased upon PA treatment (Fig. 1*D*). Adipogenic genes, such as peroxisome proliferator-activated receptor γ (*PPARγ*), *PPARγ* coactivator (*PGC1-α*), *CCAAT* enhancer-binding protein α (*C/EBPα*), and CCAAT enhancer-binding protein β (*C/EBPβ*), were also upregulated by PA treatment (Fig. 1*A*). Consistently, Oil Red O staining indicated that PA stimulated brown adipocyte differentiation (Fig. 1*E*). Taken together, these data suggest that PA effectively enhanced brown adipogenesis and increased mitochondrial mass.

PA Protects against HFD-Induced Obesity

Accumulating evidence has demonstrated that BAT activation can alleviate obesity. The results in Fig. 1 indicate that PA enhanced brown adipogenesis and increased mitochondrial mass. Therefore, we hypothesized that PA could prevent

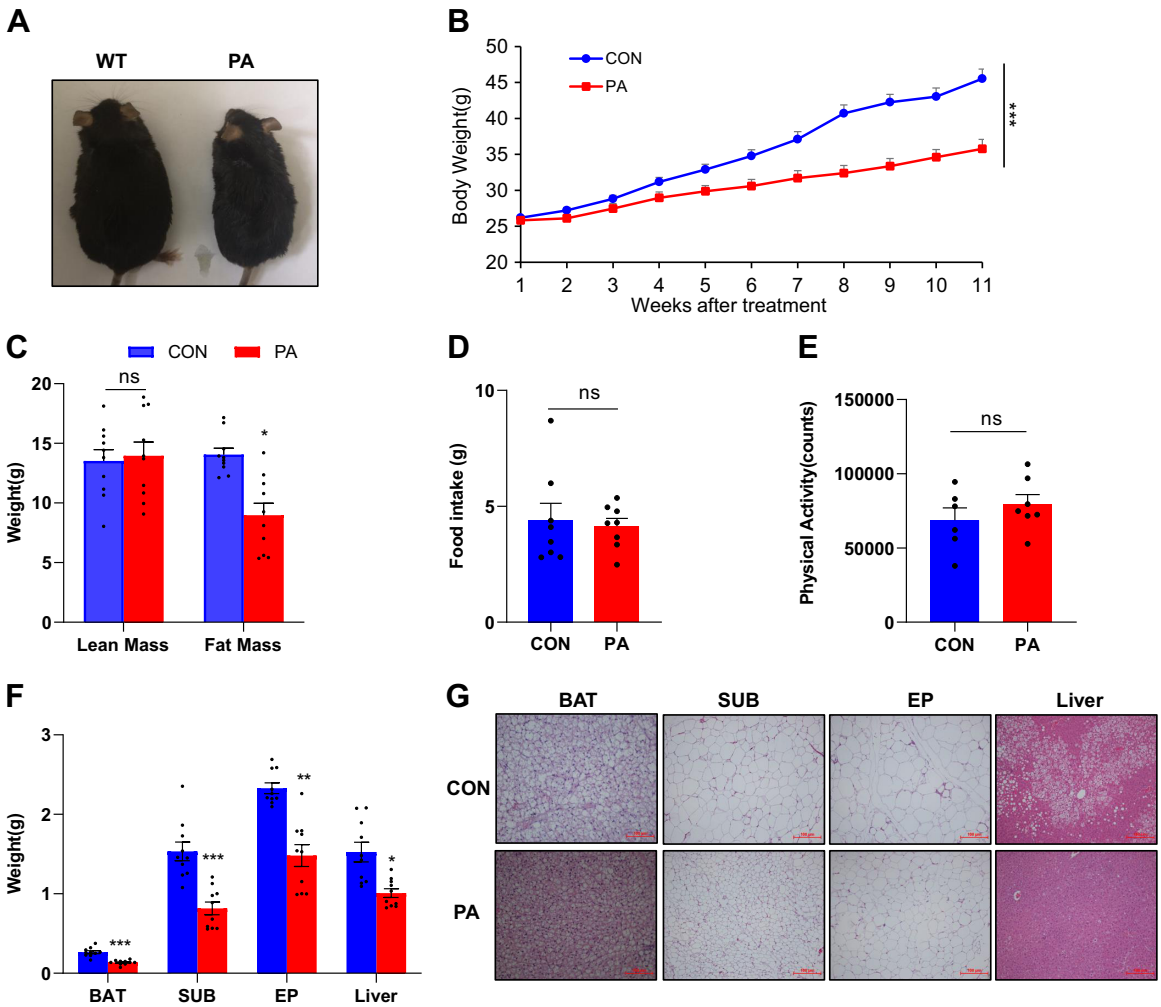

Figure 2. PA treatment resistant to HFD-induced obesity. *A* and *B*: body weight of C57/BL6 male mice treated with saline ($n = 10$) or PA (10 mg/kg, $n = 10$) fed a high-fat diet for 10 wk. *C*: NMR analysis of lean mass and fat mass of HFD mice treated with saline ($n = 10$) or PA (10 mg/kg, $n = 10$) at 15 wk of age. *D*: food intake for 48 h, saline ($n = 8$) and PA ($n = 8$). *E*: physical activity for 24 h, saline ($n = 6$) and PA ($n = 7$). *F*: tissue weight of HFD mice treated with saline ($n = 10$) or PA ($n = 10$). *G*: representative H&E staining of BAT, SUB, EP, and liver (Scale bar =100 μm). Data are shown as means ± SE. Two-tailed Student's *t* test was performed; $^{***}P < 0.001$, $^{**}P < 0.01$, and $^{*}P < 0.05$ were considered significant. BAT, brown adipose tissue; EP, epididymis adipose tissue; HFD, high-fat diet; PA, pantothenate; SUB, subcutaneous adipose tissue.

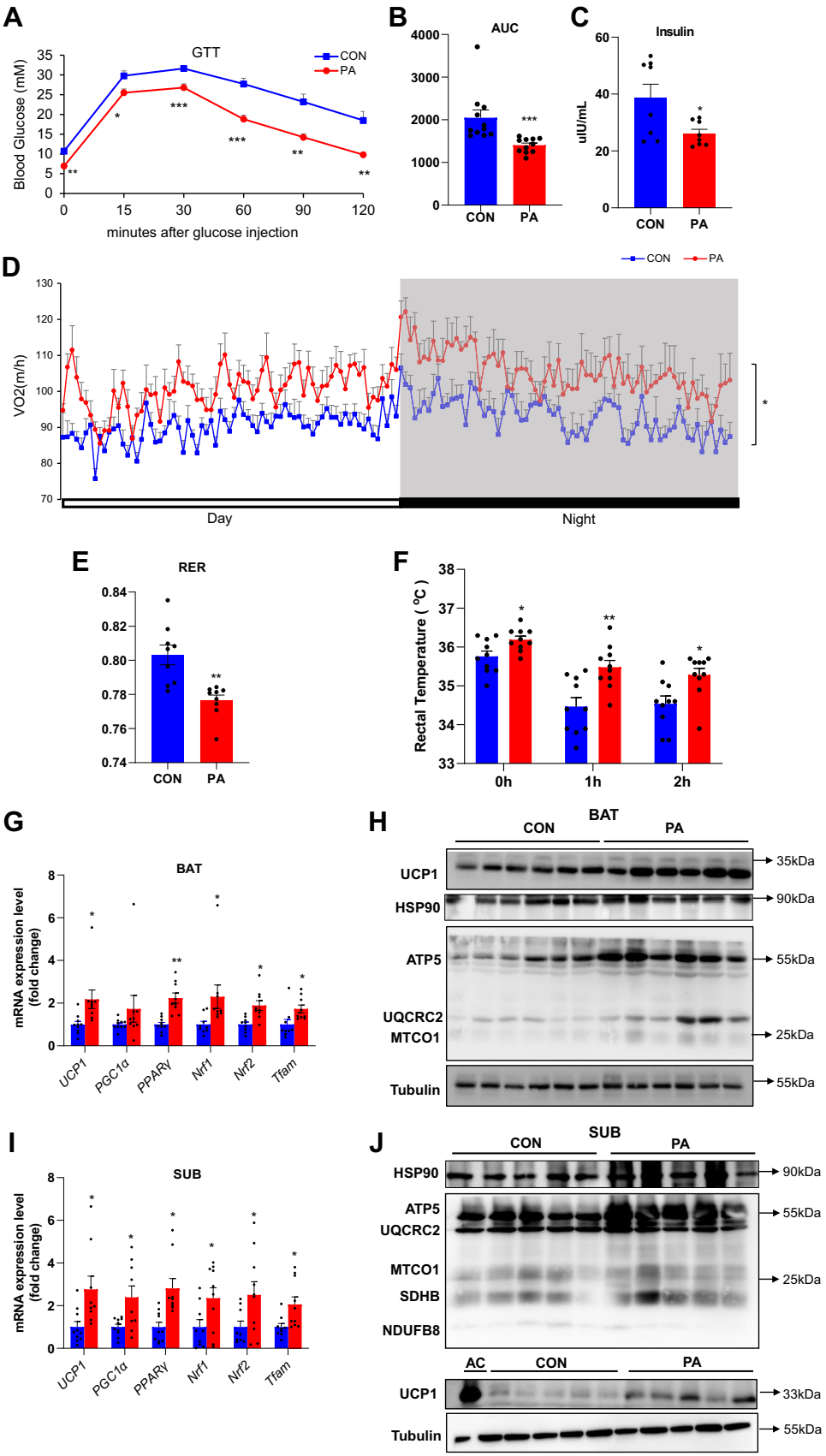

Figure 3. PA increases energy metabolism and BAT activity. *A*: glucose tolerance test of each group (injected with 1.5 g/kg after 16 h of fasting) at the age of 12 wk saline (n = 10) and PA (n = 10). *B*: average area under the curve of GTT. *C*: serum insulin concentration: saline (n = 8) and PA (n = 8). *D*: oxygen consumption rate in each group of mice aged 9 wk; (n = 9). *E*: respiratory exchange ratio (RER) of each group (n = 9). *F*: rectal temperature of each group at room (24°C) and low (4°C) temperatures for 2 h (n =10) at 15 wk of age. *G*: mRNA expression level of BAT marker genes and mitochondrial biogenic genes in BAT: saline (n = 8) and PA (n = 10). *H*: Western blot of HSP90, OXPHOS, UCP1, and tubulin expression saline in BAT: saline (n = 6) and PA (n = 6). *I*: mRNA expression level of BAT marker genes and mitochondrial biogenic genes in BAT: saline (n = 8) and PA (n = 10). *J*: Western blot of HSP90, OXPHOS, UCP1, and tubulin expression in SUB: saline (n = 5) and PA (n = 5), BAT sample stands for AC (active control). Data are shown as means ± SE. Two-tailed Student's t test was performed; $^{***}P < 0.001$, $^{**}P < 0.01$, and $^{*}P < 0.05$ were considered significant. BAT, brown adipose tissue; GTT, glucose tolerance test; HSP90, heat shock protein 90; OXPHOS, oxidative phosphorylation; PA, pantothenate; SUB, subcutaneous adipose tissue; UCP1, uncoupling protein 1.

AJP-Endocrinol Metab • doi:10.1152/ajpendo.00293.2021 • www.ajpendo.org

obesity by increasing BAT activation. To investigate this, mice fed an HFD were treated with PA (10 mg/kg) for 11 consecutive weeks. PA treatment significantly prevented HFD-induced obesity from the fifth week, compared with the control group mice (Fig. 2, *A* and *B*). Nuclear magnetic resonance (NMR) analysis revealed significantly reduced fat mass in the PA group mice, and no marked difference was observed in lean mass between the two groups (Fig. 2*C*). These results indicated that the observed reduced body weight gain in the PA group was due to reduced adiposity. The weights of BAT, subcutaneous adipose tissue (SUB), epididymis adipose tissue (EP), and liver were also significantly reduced in the PA group compared with the control group but not in other organs (Fig. 2*D* and Supplemental Fig. S3, *A* and *B*). Physical activity, food intake, and energy absorption were not significantly altered in the PA group (Fig. 2, *E* and *F*) in conjunction with indicators of sympathetic nervous system activation such as tyrosine hydroxylase (TH) and deiodinase (DIO2) (Supplemental Fig. S3, *C* and *D*). Consistently, hematoxylin and eosin (HE) analysis demonstrated that PA reduced adipocyte lipid deposition in BAT, SUB, and EP (Fig. 2*G*). Moreover, hepatic steatosis was remarkably attenuated by PA treatment (Fig. 2*G*). These results indicate that PA treatment effectively reduced HFD-induced obesity.

PA Promotes Energy Expenditure by BAT Activation and Beige Adipocytes Formation

Obesity is often accompanied by impaired glucose homeostasis. In this study, we investigated the effects of PA treatment on glucose metabolism using an intraperitoneal glucose tolerance test (GTT) after 6 wk of HFD. PA treatment significantly improved glucose tolerance compared with control vehicle treatment (Fig. 3, *A* and *B*). Consistently, serum insulin levels were significantly reduced by PA treatment (Fig. 3*C*).

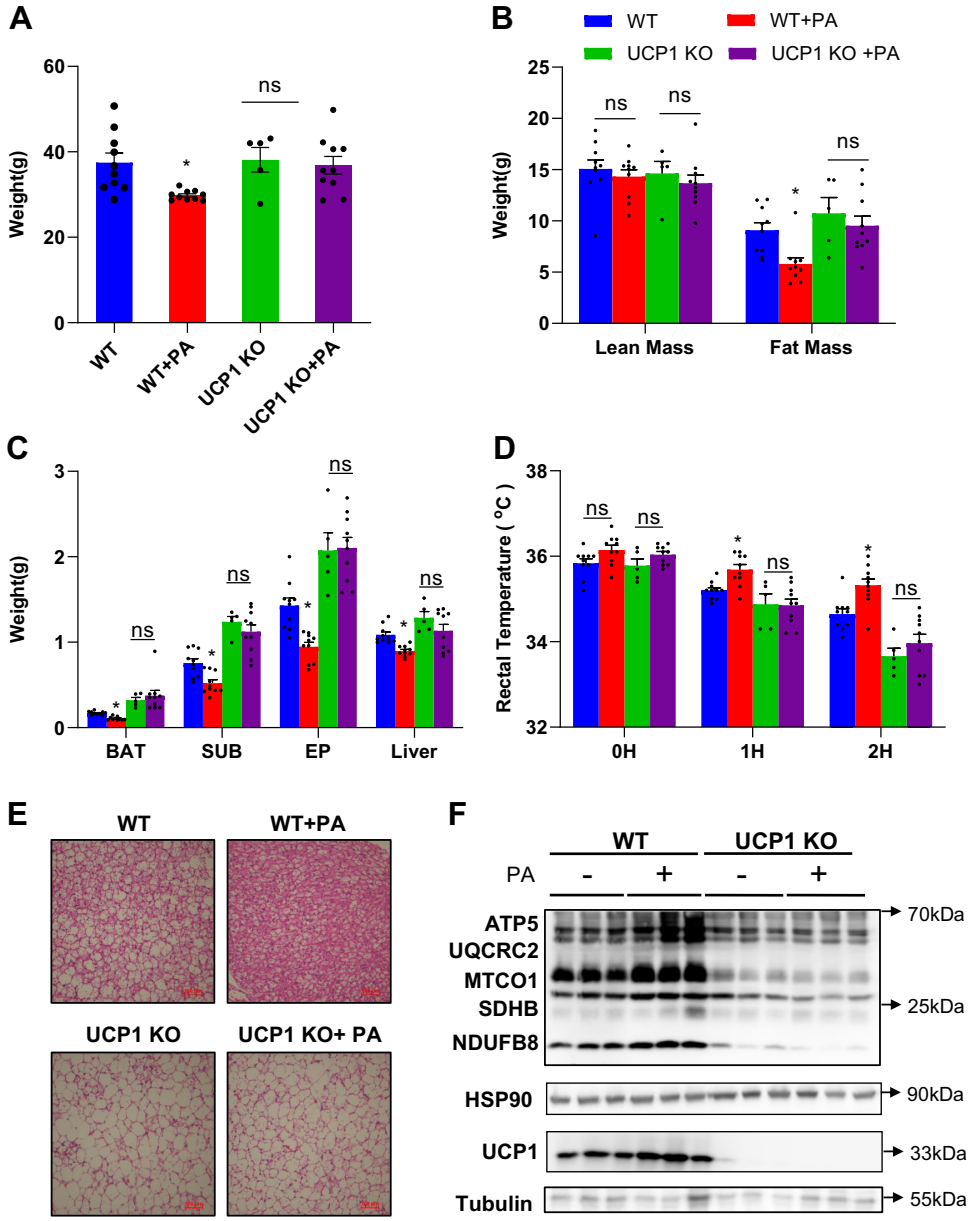

Figure 4. Antiobesity function of PA is UCP1-dependent. HFD-induced WT mice and UCP1 KO mice were treated with saline or PA (10 mg/kg) for 10 wk. *A*: body weight of mice at 13 wk of age. (n = 5–10). *B*: lean mass and fat mass of mice in each group at the age of 14 wk. (n = 5–10). *C*: tissue weight in each group. (n = 5–10). *D*: rectal temperature of each group at room (25°C) and low (4°C) temperatures for 2 h at the age of 14 wk; (n = 5–10). *E*: representative H&E staining images of BAT in each group (Scale bar =100 μm); (n = 5–10). *F*: Western blotting analysis of UCP1, OXPHOS, HSP90, and tubulin protein levels in BAT (n =3). Statistical analysis was performed by one-way repeated-measures ANOVA (*A*–*D*) with multiple comparisons and Tukey's posttest; $^{***}P < 0.001$, $^{**}P < 0.01$, and $^{*}P < 0.05$ were considered significant. BAT, brown adipose tissue; HFD, high-fat diet; HSP90, heat shock protein 90; KO, knockout; OXPHOS, oxidative phosphorylation; PA, pantothenate; SUB, subcutaneous adipose tissue; UCP1, uncoupling protein 1; WT, wild type.

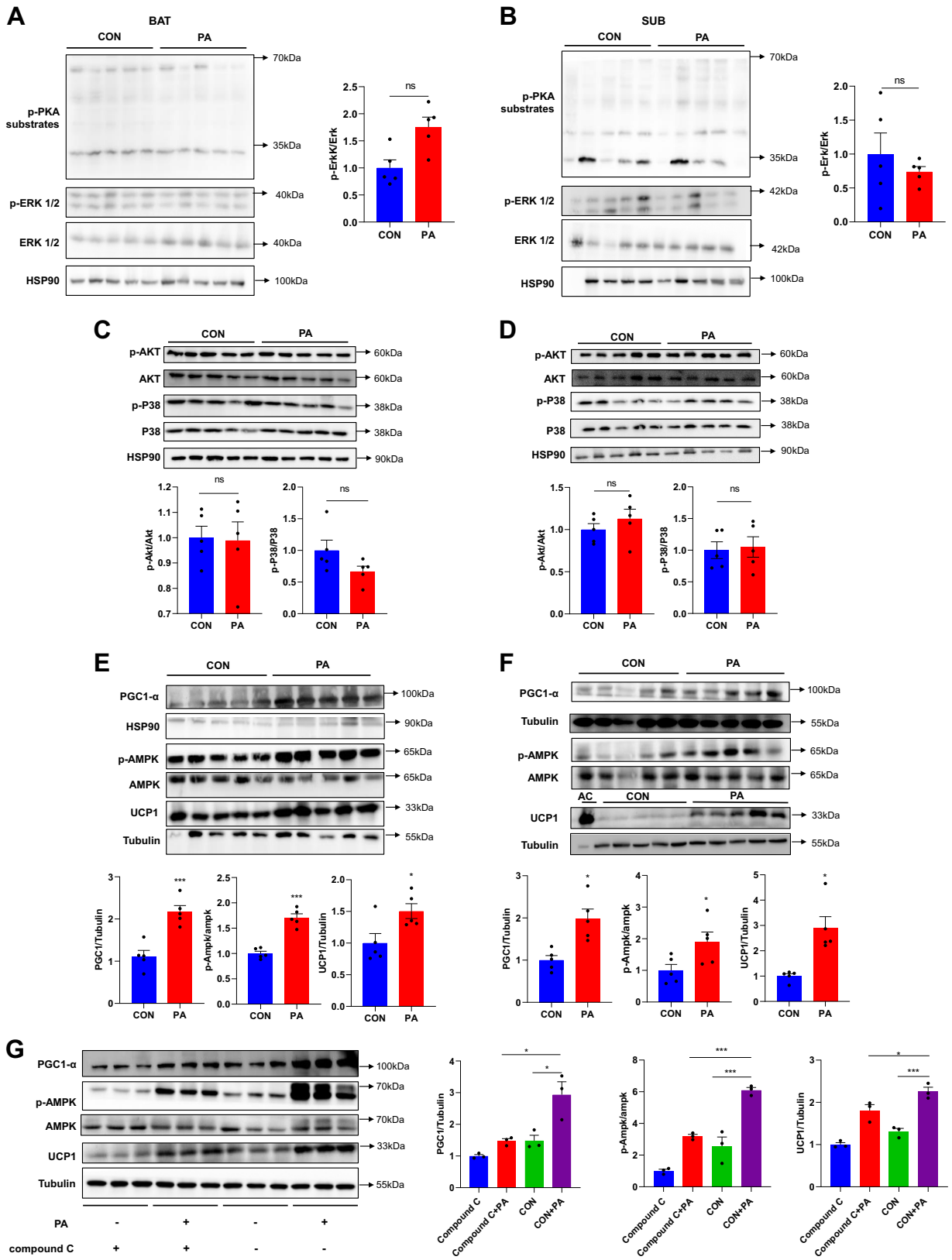

AJP-Endocrinol Metab • doi:10.1152/ajpendo.00293.2021 • www.ajpendo.org

These results strongly indicated that PA effectively maintained glucose homeostasis in mice on an HFD.

As a major nonshivering thermogenic organ, BAT plays a critical role in energy homeostasis. In this study, we examined the effects of PA treatment on energy metabolism. PA treatment significantly increased oxygen consumption and energy expenditure when the body weights were matched in the two groups (Fig. 3*D*). Moreover, the respiratory exchange ratio (RER) was dramatically reduced in PA-treated mice (Fig. 3*E*). BAT activation stimulated the oxidation of fatty acids, indicating that PA induced a shift in energy usage from oxidizing glucose to lipids. PA-treated mice exhibited a significantly higher core body temperature in response to acute cold exposure than control mice (Fig. 3*F*). These results were consistent with the observation that reduced adiposity in the PA group was due to an increase in energy expenditure (Fig. 2). Based on the aforementioned findings, we speculated that PA plays an important role in BAT function in vivo. Key genes related to BAT activity, including *UCP1*, *PPARγ2*, *TFAM*, *NRF1*, and *NRF2*, were significantly increased by PA treatment (Fig. 3*G* and Supplemental Fig. S2*B*). Consistently, the protein expression levels of UCP1 and oxidative phosphorylation (OXPHOS)-related proteins and CS activity were significantly upregulated in the BAT of PA-treated mice (Fig. 3*H*, Supplemental Fig. S4*A*). We also observed a beige-like adipocyte formation in SUB after PA treatment, which was consistent with the marked increase in the thermogenic genes, including *UCP1*, *PGC1α*, *PPARγ2*, *TFAM*, *NRF1*, and *NRF2* (Fig. 3*I* and Supplemental Fig. S2*C*) at the mRNA level, and UCP1 and OXPHOS expression at the protein level, as well as the increased CS activity (Fig. 3*J*, Supplemental Fig. S4*B*). These results strongly suggested that PA promotes energy expenditure by BAT activation and beige adipocyte formation.

The effect of PA was also evaluated at thermoneutral conditions (30°C), which reduces sympathetic activation of BAT. We found that PA treatment did not significantly reduce weight gain in mice fed a normal chow diet under thermoneutral conditions (Supplemental Fig. S5*A*); however, PA treatment still reduced HFD-induced weight gain (Supplemental Fig. S5*B*). At thermoneutral conditions, the induction of thermogenesis by the adrenergic agonist CL 316,243 was BAT dominant and raised the requirement for BAT thermogenesis (33). Acute CL 316,243 injection revealed a greater capacity for nonshivering thermogenesis, indicated as core body temperature in both PA-treated mice fed with chow or HFD (Supplemental Fig. S5, *C* and *D*), which was consistent with the increased UCP1 content (Supplemental Fig. S5, *E* and *F*). These results revealed that PA treatment retained the BAT activity under thermoneutral conditions. Surprisingly, we found that oxygen consumption was slightly increased in PA-treated chow-fed, but not HFD-fed mice (Supplemental Fig. S5, *G* and *H*). In addition, CL316,243 further enhanced PA-stimulated oxygen expenditure in PA-treated chow-fed but in not HFD-fed mice (Supplemental Fig. S5, *G* and *H*). Collectively, these data support that PA could significantly stimulate BAT activity and finally reduce obesity.

PA Functions in a UCP1-Dependent Manner

As UCP1 is a critical factor of the energy expenditure in BAT, UCP1 KO mice were used to assess the crucial role of PA in BAT function. PA treatment significantly reduced the body weight of WT mice, but not UCP1 KO mice (Fig. 4*A*). Consistently, PA treatment significantly reduced the fat mass of WT mice, but not of UCP1 KO mice (Fig. 4, *B* and *C*). In addition, PA treatment significantly increased the rectal temperature of WT mice but not of UCP1 KO mice (Fig. 4*D*). Furthermore, the histological analysis showed that the lipid deposition was reduced significantly with PA treatment in WT but not UCP1 KO mice (Fig. 4*E*). Accordingly, protein expression of UCP1 and OXPHOS in BAT was upregulated by PA treatment in WT but not UCP1 KO mice (Fig. 4*F*). These data suggest that the beneficial effects of PA are mediated by UCP1. It is of interest to explore the mechanisms by which PA treatment upregulates the expression of UCP1. Thus, the well-known pathways that mediate UCP1 expression were examined in mice fed an HFD for 4 wk. The phosphorylation levels of p38, extracellular-signal-regulated kinase 1/2 (ERK1/2), and phosphorylation of protein kinase A (PKA) substrates were not significantly affected in either BAT or SUB (Fig. 5, *A*–*D*). Interestingly, the phosphorylation of AMP-activated protein kinase (AMPK) was significantly increased in both BAT and SUB (Fig. 5, *E* and *F*). The phosphorylation of AMPK recruits PGC1α to the UCP1 promoter region, inducing UCP1 expression in BAT and SUB (30, 31). We then investigated the potential role of AMPK in PA-induced UCP1 expression. It has been reported that compound C can partially inhibit phosphorylation of AMPK as well as bone morphogenetic protein, Akt, and MAPK signaling pathways (34, 35). We found that compound C inhibited partially the increase in UCP1 induced by PA (Fig. 5*G*). Therefore, we speculate that there should exist other signaling pathways in combination with AMPK to contribute to the PA-induced UCP1 upregulation. Taken together, these results demonstrate that PA functions in a UCP1-dependent manner.

Figure 5. Signaling pathways of PA. *A*: Western blot of phosphorylation of PKA, phosphorylation of ERK1/2, total ERK1/2, and HSP90 in BAT ($n = 5$). Blots densitometry were quantified ($n = 5$). *B*: Western blot of phosphorylation of PKA, phosphorylation of ERK1/2, total ERK1/2, and HSP90 in SUB ($n = 5$). Blots densitometry were quantified ($n = 5$). *C*: Western blot of phosphorylation of AKT, total AKT, phosphorylation of P38, total P38, and HSP90 in BAT ($n = 5$). Blot densitometry was quantified below the blots ($n = 5$). *D*: Western blot of phosphorylation of AKT, total AKT, phosphorylation of P38, total P38, and HSP90 in SUB ($n = 5$). Blot densitometry was quantified below the blots ($n = 5$). *E*: Western blot of PGC1-α, HSP90, phosphorylation of AMPK, total AMPK, UCP1, and tubulin in BAT ($n = 5$). Blot densitometry was quantified below the blots ($n = 5$). *F*: Western blot of PGC1–α, HSP90, phosphorylation of AMPK, total AMPK, UCP1, and tubulin in SUB ($n = 5$). BAT sample stands for AC (active control). Blot densitometry was quantified below the blots ($n = 5$). *G*: Western blot of PGC1–α, phosphorylation of AMPK, total AMPK, UCP1, and tubulin in differentiated brown adipocytes on D6 with or without of PA (5 μM), compound C (500 μM) for 2 h ($n = 3$). Blot densitometry was quantified below the blots ($n = 3$). For blot densitometry, data are shown as means ± SE. Two-tailed Student's *t* test was performed (*A*–*F*); statistical analysis was performed by one-way repeated-measures ANOVA (*G*) with multiple comparisons and Tukey's posttest; $^{***}P < 0.001$, $^{**}P < 0.01$, and $^{*}P < 0.05$ were considered significant. AMPK, AMP-activated protein kinase; BAT, brown adipose tissue; ERK1/2, extracellular-signal-regulated kinase 1/2; HSP90, heat shock protein 90; PA, pantothenate; PGC1-α, *PPARγ* coactivator; PKA, protein kinase A; SUB, subcutaneous adipose tissue; UCP1, uncoupling protein 1.

DISCUSSION

To our knowledge, this is the first study to report that PA acts as a BAT activator with significant beneficial effects on obesity. PA treatment activated BAT and enhanced energy expenditure, resulting in significantly reduced adiposity, improved hepatic steatosis, and improved glucose homeostasis in HFD-fed mice. Using a UCP1 KO mouse model combined with HFD treatment, we demonstrated that the metabolic beneficial effects of PA are mediated by UCP1. Together, these results revealed the critical mechanism of the PA-BAT-UCP1 axis in obesity treatment.

PA has a long history of being widely used as a clinical drug, health supplement, and food additive, and multiple beneficial effects of PA on lipid metabolism have been reported (27). However, its target organ and detailed mechanisms have remained elusive. PA is reported as a precursor of CoA, and protects against the harmful effects of caloric overload in Drosophila (25), further supporting our finding that PA has a beneficial effect on lipid metabolism. In this study, PA induced primary adipocytes to acquire a "brown-like" phenotype, and partially activated the AMPK-PGC1α-UCP1 pathway. AMPK phosphorylation triggers catabolic metabolism and improves mitochondrial biogenesis (36). Consistently, PA treatment significantly increased mitochondrial mass both in vivo and in vitro. However, further study is needed to investigate the detailed interaction of PA with the AMPK subunit and their roles in mitochondrial biogenesis and function.

BAT activation can stimulate adaptive thermogenesis by UCP1, which uncouples mitochondrial proton gradient from ATP synthesis increasing heat production and energy expenditure (37). Our group has previously shown that an increase in the BAT mass via BAT transplantation prevented obesity development (38). In this study, PA was screened and identified as an effective BAT-activating factor that increases energy metabolism. The possibilities that PA may function via β3-adrenergic activation were excluded as food intake, physical activity, and indicators of activated sympathetic nerves, such as TH and DIO2 were not changed. At thermoneutral conditions, PA treatment could still prevent HFD-induced body weight gain, suggesting that the antiobesity effects of PA are independent of the sympathetic nervous system. Notably, a recent study also showed that BAT activation by phytochemical hyperforin significantly increased energy expenditure in a sympathetic nerve system-independent manner (39).

As a member of the vitamin B family, PA is a natural acetyl-CoA metabolite in lipid metabolism. No significant PA toxicity has been found in the present study at a dosage of 10 mg/kg/day, although higher doses (>10 g/day) may cause mild intestinal distress or diarrhea (27). Safety and effective strategies for weight loss are a major research trend, and a more detailed and direct toxicology trial with PA treatment will be conducted in the future. The current study provides data indicating that PA is a safe and promising candidate for BAT activation, with potential value as an antiobesity drug.

In addition, this study does not exclude the possibility that PA may play a beneficial role in other organs in addition to BAT, such as in the context of intestinal flora, and the gut barrier (40, 41).

In conclusion, this study demonstrated that PA activates BAT to reduce obesity and improve hepatic steatosis and glucose homeostasis in a UCP1-dependent manner. Thus, PA could be a promising target for treating obesity and related disease.

SUPPLEMENTAL DATA

Supplemental Figs. S1–S5: https://doi.org/10.6084/m9.figshare.15180819.

GRANTS

This work was supported by the General Program (Major Research Plan) of National Natural Science Foundation of China (92057208), Youth Program of National Natural Science Foundation of China (31900830), the National Natural Science Foundation of China (81770834, 81770577, and 82170591), China Postdoctoral Science Foundation (2021T140665), and the National Key Research and Development Program of China (2017YFC1001003).

DISCLOSURES

No conflicts of interest, financial or otherwise, are declared by the authors.

AUTHOR CONTRIBUTIONS

H. Zhou, H. Zhang, R.Y., J.L., M.D., and W.J. conceived and designed research; H. Zhou, H.Zhang, R.Y., C.Y., Y.H., X.J., S.Y., L.C., R.J., Z.C., and Z.Z. performed experiments; H. Zhou, H. Zhang, and K.Z. analyzed data; H.Z. interpreted results of experiments; H. Zhou and C.Y. prepared figures; H. Zhou drafted manuscript; H.Zhou, H.Zhang, R.Y., C.Y., and W.J. edited and revised manuscript; H. Zhou, H.Zhang, R.Y., C.Y., J.L., Y.H., X.J., S.Y., L.C., R.J., K.Z., Z.C., Z.Z., M.D., and W.J. approved final version of manuscript.

REFERENCES

1. **Nicolaidis S.** Environment and obesity. *Metabolism* 100S: 153942, 2019. doi:10.1016/j.metabol.2019.07.006.
2. **Esser N**, **Legrand-Poels S**, **Piette J**, **Scheen AJ**, **Paquot N.** Inflammation as a link between obesity, metabolic syndrome and type 2 diabetes. *Diabetes Res Clin Pract* 105: 141–150, 2014. doi:10.1016/j.diabres.2014.04.006.
3. **Vecchié A**, **Dallegri F**, **Carbone F**, **Bonaventura A**, **Liberale L**, **Portincasa P**, **Frühbeck G**, **Montecucco F.** Obesity phenotypes and their paradoxical association with cardiovascular diseases. *Eur J Intern Med* 48: 6–17, 2018. doi:10.1016/j.ejim.2017.10.020.
4. **Seravalle G**, **Grassi G.** Obesity and hypertension. *Pharmacol Res* 122: 1–7, 2017. doi:10.1016/j.phrs.2017.05.013.
5. **Yuan X**, **Hu T**, **Zhao H**, **Huang Y**, **Ye R**, **Lin J**, **Zhang C**, **Zhang H**, **Wei G**, **Zhou H**, **Dong M**, **Zhao J**, **Wang H**, **Liu Q**, **Lee HJ**, **Jin W**, **Chen ZJ.** Brown adipose tissue transplantation ameliorates polycystic ovary syndrome. *Proc Natl Acad Sci USA* 113: 2708–2713, 2016. doi:10.1073/pnas.1523236113.
6. **Avgerinos KI**, **Spyrou N**, **Mantzoros CS**, **Dalamaga M.** Obesity and cancer risk: emerging biological mechanisms and perspectives. *Metabolism* 92: 121–135, 2019. doi:10.1016/j.metabol.2018.11.001.
7. **Nieto-Martínez R**, **González-Rivas JP**, **Lima-Martínez M**, **Stepenka V**, **Rísquez A**, **Mechanick JI.** Diabetes care in Venezuela. *Ann Glob Health* 81: 776–791, 2015. doi:10.1016/j.aogh.2015.11.002.
8. **Srivastava G**, **Apovian CM.** Current pharmacotherapy for obesity. *Nat Rev Endocrinol* 14: 12–24, 2018. doi:10.1038/nrendo.2017.122.
9. **Paccosi S**, **Cresci B**, **Pala L**, **Rotella CM**, **Parenti A.** Obesity therapy: how and why? *Curr Med Chem* 27: 174–186, 2020. doi:10.2174/0929867326666190124121725.

10. **Wirth A**, **Wabitsch M**, **Hauner H.** The prevention and treatment of obesity. *Dtsch Arztebl Int* 111: 705–713, 2014. doi:10.3238/arztebl.2014.0705.
11. **Marlatt KL**, **Ravussin E.** Brown adipose tissue: an update on recent findings. *Curr Obes Rep* 6: 389–396, 2017. doi:10.1007/s13679-017-0283-6.
12. **Lidell ME**, **Enerbäck S.** Brown adipose tissue–a new role in humans? *Nat Rev Endocrinol* 6: 319–325, 2010. doi:10.1038/nrendo.2010.64.
13. **Hanssen MJ**, **Hoeks J**, **Brans B**, **van der Lans AA**, **Schaart G**, **van den Driessche JJ**, **Jörgensen JA**, **Boekschoten MV**, **Hesselink MK**, **Havekes B**, **Kersten S**, **Mottaghy FM**, **van Marken Lichtenbelt WD**, **Schrauwen P.** Short-term cold acclimation improves insulin sensitivity in patients with type 2 diabetes mellitus. *Nat Med* 21: 863–865, 2015. doi:10.1038/nm.3891.
14. **Hankir MK**, **Kranz M**, **Keipert S**, **Weiner J**, **Andreasen SG**, **Kern M**, **Patt M**, **Klöting N**, **Heiker JT**, **Brust P**, **Hesse S**, **Jastroch M**, **Fenske WK.** Dissociation between brown adipose tissue ^{18}F-FDG uptake and thermogenesis in uncoupling protein 1-deficient mice. *J Nucl Med* 58: 1100–1103, 2017. doi:10.2967/jnumed.116.186460.
15. **Okla M**, **Kim J**, **Koehler K**, **Chung S.** Dietary factors promoting brown and beige fat development and thermogenesis. *Adv Nutr* 8: 473–483, 2017. doi:10.3945/an.116.014332.
16. **Shabalina IG**, **Petrovic N**, **de Jong JM**, **Kalinovich AV**, **Cannon B**, **Nedergaard J.** UCP1 in brite/beige adipose tissue mitochondria is functionally thermogenic. *Cell Rep* 5: 1196–1203, 2013. doi:10.1016/j.celrep.2013.10.044.
17. **Chouchani ET**, **Kazak L**, **Spiegelman BM.** New advances in adaptive thermogenesis: UCP1 and beyond. *Cell Metab* 29: 27–37, 2019. doi:10.1016/j.cmet.2018.11.002.
18. **Quan LH**, **Zhang C**, **Dong M**, **Jiang J**, **Xu H**, **Yan C**, **Liu X**, **Zhou H**, **Zhang H**, **Chen L**, **Zhong FL**, **Luo ZB**, **Lam SM**, **Shui G**, **Li D**, **Jin W.** Myristoleic acid produced by enterococci reduces obesity through brown adipose tissue activation. *Gut* 69: 1239–1247, 2020. doi:10.1136/gutjnl-2019-319114.
19. **Yuan X**, **Wei G**, **You Y**, **Huang Y**, **Lee HJ**, **Dong M**, **Lin J**, **Hu T**, **Zhang H**, **Zhang C**, **Zhou H**, **Ye R**, **Qi X**, **Zhai B**, **Huang W**, **Liu S**, **Xie W**, **Liu Q**, **Liu X**, **Cui C**, **Li D**, **Zhan J**, **Cheng J**, **Yuan Z**, **Jin W.** Rutin ameliorates obesity through brown fat activation. *FASEB J* 31: 333–345, 2017. doi:10.1096/fj.201600459RR.
20. **Hu T**, **Yuan X**, **Wei G**, **Luo H**, **Lee HJ**, **Jin W.** Myricetin-induced brown adipose tissue activation prevents obesity and insulin resistance in db/db mice. *Eur J Nutr* 57: 391–403, 2018. doi:10.1007/s00394-017-1433-z.
21. **Said HM.** Water-soluble vitamins. *World Rev Nutr Diet* 111: 30–37, 2015. doi:10.1159/000362294.
22. **Pett HE**, **Jansen PA**, **Hermkens PH**, **Botman PN**, **Beuckens-Schortinghuis CA**, **Blaauw RH**, **Graumans W**, **van de Vegte-Bolmer M**, **Koolen KM**, **Rutjes FP**, **Dechering KJ**, **Sauerwein RW**, **Schalkwijk J.** Novel pantothenate derivatives for anti-malarial chemotherapy. *Malar J* 14: 169, 2015. doi:10.1186/s12936-015-0673-8.
23. **Sanvictores T**, **Chauhan S.** Vitamin B5 (pantothenic acid). In: *StatPearls*. Treasure Island, FL: StatPearls Publishing, 2022.
24. **Naruta E**, **Buko V.** Hypolipidemic effect of pantothenic acid derivatives in mice with hypothalamic obesity induced by aurothioglucose. *Experimental and toxicologic pathology: official journal of the Gesellschaft fur. Exp Toxicol Pathol* 53: 393–398, 2001. doi:10.1078/0940-2993-00205.
25. **Palanker Musselman L**, **Fink JL**, **Baranski TJ.** CoA protects against the deleterious effects of caloric overload in Drosophila. *J Lipid Res* 57: 380–387, 2016. doi:10.1194/jlr.M062976.
26. **Meyer CW**, **Willershauser M**, **Jastroch M**, **Rourke BC**, **Fromme T**, **Oelkrug R**, **Heldmaier G**, **Klingenspor M.** Adaptive thermogenesis and thermal conductance in wild-type and UCP1-KO mice. *Am J Physiol Regul Integr Comp Physiol* 299: R1396–R1406, 2010. doi:10.1152/ajpregu.00021.2009.
27. **Chawla J**, **Kvarnberg D.** Hydrosoluble vitamins. *Handb Clin Neurol* 120: 891–914, 2014. doi:10.1016/B978-0-7020-4087-0.00059-0.
28. **Wu NN**, **Zhang CH**, **Lee HJ**, **Ma Y**, **Wang X**, **Ma XJ**, **Ma W**, **Zhao D**, **Feng YM.** Brown adipogenic potential of brown adipocytes and peri-renal adipocytes from human embryo. *Sci Rep* 6: 39193, 2016. doi:10.1038/srep39193.
29. **Chi QS**, **Wang DH.** Thermal physiology and energetics in male desert hamsters (Phodopus roborovskii) during cold acclimation. *J Comp Physiol B* 181: 91–103, 2011. doi:10.1007/s00360-010-0506-6.
30. **Yin N**, **Zhang H**, **Ye R**, **Dong M**, **Lin J**, **Zhou H**, **Huang Y**, **Chen L**, **Jiang X**, **Nagaoka K**, **Zhang C**, **Jin W.** Fluvastatin sodium ameliorates obesity through brown fat activation. *Int J Mol Sci* 20: 1622, 2019. doi:10.3390/ijms20071622.
31. **Ludy MJ**, **Moore GE**, **Mattes RD.** The effects of capsaicin and capsiate on energy balance: critical review and meta-analyses of studies in humans. *Chem Senses* 37: 103–121, 2012. doi:10.1093/chemse/bjr100.
32. **Caşcaval D**, **Poştaru M**, **Kloetzer L**, **Blaga AC**, **Galaction AI.** *Chemical Stability of Vitamin B5*. Cham: Springer International Publishing, 2017, p. 341–344.
33. **Cannon B**, **Nedergaard J.** Brown adipose tissue: function and physiological significance. *Physiol Rev* 84: 277–359, 2004. doi:10.1152/physrev.00015.2003.
34. **Zhang Z**, **Zhang H**, **Li B**, **Meng X**, **Wang J**, **Zhang Y**, **Yao S**, **Ma Q**, **Jin L**, **Yang J**, **Wang W**, **Ning G.** Berberine activates thermogenesis in white and brown adipose tissue. *Nat Commun* 5: 5493, 2014. doi:10.1038/ncomms6493.
35. **Puigserver P**, **Wu Z**, **Park CW**, **Graves R**, **Wright M**, **Spiegelman BM.** A cold-inducible coactivator of nuclear receptors linked to adaptive thermogenesis. *Cell* 92: 829–839, 1998. doi:10.1016/s0092-8674(00)81410-5.
36. **Wang Y**, **An H**, **Liu T**, **Qin C**, **Sesaki H**, **Guo S**, **Radovick S**, **Hussain M**, **Maheshwari A**, **Wondisford FE**, **O'Rourke B**, **He L.** Metformin improves mitochondrial respiratory activity through activation of AMPK. *Cell Rep* 29: 1511–1523.e5, 2019. doi:10.1016/j.celrep.2019.09.070.
37. **Roesler A**, **Kazak L.** UCP1-independent thermogenesis. *Biochem J* 477: 709–725, 2020. doi:10.1042/BCJ20190463.
38. **Liu X**, **Wang S**, **You Y**, **Meng M**, **Zheng Z**, **Dong M**, **Lin J**, **Zhao Q**, **Zhang C**, **Yuan X**, **Hu T**, **Liu L**, **Huang Y**, **Zhang L**, **Wang D**, **Zhan J**, **Jong Lee H**, **Speakman JR**, **Jin W.** Brown adipose tissue transplantation reverses obesity in Ob/Ob mice. *Endocrinology* 156: 2461–2469, 2015. doi:10.1210/en.2014-1598.
39. **Chen S**, **Liu X**, **Peng C**, **Tan C**, **Sun H**, **Liu H**, **Zhang Y**, **Wu P**, **Cui C**, **Liu C**, **Yang D**, **Li Z**, **Lu J**, **Guan J**, **Ke X**, **Wang R**, **Bo X**, **Xu X**, **Han J**, **Liu J.** The phytochemical hyperforin triggers thermogenesis in adipose tissue via a Dlat-AMPK signaling axis to curb obesity. *Cell Metab* 33: 565–580.e7, 2021. doi:10.1016/j.cmet.2021.02.007.
40. **Everard A**, **Belzer C**, **Geurts L**, **Ouwerkerk JP**, **Druart C**, **Bindels LB**, **Guiot Y**, **Derrien M**, **Muccioli GG**, **Delzenne NM**, **de Vos WM**, **Cani PD.** Cross-talk between Akkermansia muciniphila and intestinal epithelium controls diet-induced obesity. *Proc Natl Acad Sci USA* 110: 9066–9071, 2013. doi:10.1073/pnas.1219451110.
41. **Patterson E**, **Ryan PM**, **Cryan JF**, **Dinan TG**, **Ross RP**, **Fitzgerald GF**, **Stanton C.** Gut microbiota, obesity and diabetes. *Postgrad Med J* 92: 286–300, 2016. doi:10.1136/postgradmedj-2015-133285.